Progress In Electromagnetics Research C, Vol. 63, 43–51, 2016

Ka-Band Low Profile Circularly Polarized Reflectarray

Abdelhady Mahmoud[1, *] and Ahmed A. Kishk[2]

Abstract—Single-layer circularly polarized (CP) reflectarrays in the Ka-band are presented in this paper. Three reflectarray (RA) models are designed and measured, using geometrically dissimilar elements. Each element is analyzed individually and optimized to obtain good performance within the operating frequency band. To compensate the spatial delay from feed to the elements at RA surface, the angular rotation technique has been employed for obtaining reflected phase curve. The performances of the antennas are analyzed at 30 GHz, exhibiting 13.3% of 1.5 dB gain bandwidth, while the axial ratio bandwidth is less than 3 dB in the whole operating band.

1. INTRODUCTION

In satellite communications, the circularly polarized (CP) antenna has been chosen widely because of its robustness against environmental interference [1]. So, a variety of CP reflectarrays have been proposed in the literature using LP feeder [2–8] and CP feeder [9–15]. A reflectarrays using linearly polarized feed can be used where its polarization runs parallel to the diagonal line of the square cell element by tilting the feed by 45°, and its linearly polarized field is decomposed into two equal components along the sides of the square cell. Then, the field with the necessary phase shift of each component is recruited to attain a CP focused beam. Some of these elements such as cross slot patch [2], patch [3, 4], aperture coupled patch with slot and line of variable length [5], cross slot dielectric resonator, cross strip aperture coupled dielectric resonator [6], dual-layer T-shaped element [7], and cross dielectric resonators supported on ground [8]. The orthogonal slot lengths, patch length and width, strip line lengths, dual-layer T-shaped element arm lengths and cross dielectric resonators lengths are adjusted to achieve the required 90° phase difference between the two reflected waves. This technique has severe drawbacks such as practical adjustment of the feed diagonally with respect to the array center. In addition, since the cell is designed with two orthogonal parts having phase difference 90° at the designed frequency only, the CP behavior of unit cell reflected wave will only cover a narrowband. As a result, the overall reflectarray has a narrowband 3 dB axial ratio [3–6]. Another technique, the angular rotation, has been applied to overcome these problems. It is used to attain the phase delay for the CP reflectarrays. One essential condition of this technique is that the primary source must be a CP feed antenna based on the following principle. The element rotation technique for designing CP reflectarray was first reported by Huang and Pogorzelski [9], where the patch element is connected with two orthogonal microstrip delay lines of different lengths. Later, an element of the split ring structure was developed by Han et al. [10] and Strassner et al. [11] for simplifying the CP element structure. The reversal of polarization due to the ground plane is canceled out by the presence of these CP elements, and an element rotation of $\Delta\Phi$ results in a $2\Delta\Phi$ phase delay of the backscattering. Moreover, each element has the same dimensions and same resonant frequency. Commonly employed elements are short-circuited circular discs [12] and single-layer split square-ring elements [13]. For improving the band of CP reflectarray,

Received 5 February 2016, Accepted 20 March 2016, Scheduled 13 April 2016

* Corresponding author: Abdelhady Mahmoud (abdoeng78@gmail.com).

[1] Electrical Department, Benha Faculty of Engineering, Benha University, Benha, Egypt. [2] Department of Electrical and Computer Engineering, Concordia University, Montreal, Quebec, Canada.

a realized single-layer multiple-resonance structure to design two broadband CP reflectarray elements was introduced [14]. A double-layer cross slot supported by perforated edges DRA was analyzed with proper gain, bandwidth [15]. Here, single-layer economical CP reflectarrays are analyzed and fabricated using printed circuit technique with broadband axial ratio and suitable side lobe level.

2. ANGULAR ROTATION PRINCIPLE

Consider the case, as shown in Fig. 1(a) where reflectarray cells are assumed cross strips having two unequal arms lengths L_x and L_y.

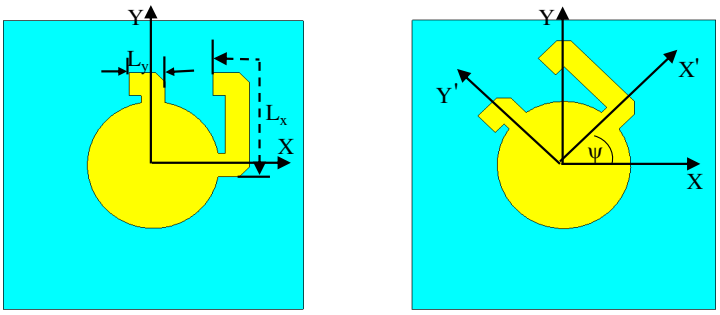

Figure 1. CP reflectarray cell disk patch loaded by two unequal stub lengths. (a) Slot with 0 degree phase shift. (b) Rotated strip with 2ψ degrees phase shift.

Let's consider that the two stubs are short-circuit terminated and let the reflectarray be illuminated by normally incident LHCP plane wave propagating in the negative z direction. This incident wave may be expressed as:

$$\vec{E}^{inc} = (\hat{u}_x + j\hat{u}_y)\, ae^{-jkz}e^{-j\omega t} \tag{1}$$

$$\vec{E}^{refl} = \left(-\hat{u}_x e^{2jkL_x} - j\hat{u}_y e^{2jkL_y}\right) ae^{jkz}e^{-j\omega t} \tag{2}$$

where the minus signs arise from the reflection coefficients of unity magnitude at the short-circuit terminations. The amplitude a is the incidence amplitude, but the attenuation is assumed zero in the strip arms. While incident waves are assumed LHCP, so as a result of ground plane, the reflected waves are RHCP. Now, the crossed strip arms with L_x and L_y are chosen so that the phase difference between the two arms is 90°, i.e., $kL_x - kL_y = \pi/2$, then the reflected waves will be:

$$\vec{E}^{refl} = e^{2jkL_y}\,(\hat{u}_x - j\hat{u}_y)\, ae^{jkz}e^{-j\omega t} \tag{3}$$

which are LHCP waves just as the incident waves.

Now let the crossed strip rotated by an angle ψ [shown in Fig. 1(b)] to be aligned with the axes of the new coordinate system (x', y'). The excitation of each of the two orthogonal component fields can be determined by projecting the $\hat{u}_x$ and $\hat{u}_y$ field components onto the $\hat{u}_{x'}$ and $\hat{u}_{y'}$ axes at $z = 0$. That is:

$$\vec{E}^{inc}_{z=0} = \left[\left(\hat{u}_{x'}\cos\psi - \hat{u}_{y'}\sin\psi\right) + j\left(\hat{u}_{x'}\sin\psi + \hat{u}_{y'}\cos\psi\right)\right] ae^{-j\omega t} = \left(\hat{u}_{x'}e^{j\psi} + j\hat{u}_{y'}e^{j\psi}\right) ae^{-j\omega t} \tag{4}$$

Now, the reflected waves become

$$\vec{E}^{refl} = -\left(\hat{u}_{x'}e^{2jkL_{x'}} + j\hat{u}_{y'}e^{2jkL_{y'}}\right) ae^{jkz}e^{j\psi}e^{-j\omega t}e^{2jkL_y} \tag{5}$$

where, again, the minus sign arises from the reflections at the short-circuit terminations (ground plane). The reflected field in terms of the original x and y components yields:

$$\vec{E}^{refl} = -\left[\left(\hat{u}_x\cos\psi + \hat{u}_y\sin\psi\right)e^{2jkL_{x'}} + j\left(-\hat{u}_x\sin\psi + \hat{u}_y\cos\psi\right)e^{2jkL_{y'}}\right] ae^{jkz}e^{-j\omega t}e^{j\psi}e^{2jkL_{y'}} \tag{6}$$

After some manipulation

$$\vec{E}^{refl} = -\frac{1}{2}\left[\left(e^{2jkL_{x'}} - e^{2jkL_{y'}}\right)(\hat{u}_x - j\hat{u}_y)\, e^{2j\psi} + \left(e^{2jkL_{x'}} + e^{2jkL_{y'}}\right)(\hat{u}_x + j\hat{u}_y)\right] a e^{jkz} e^{-j\omega t} e^{2jkL_y} \quad (7)$$

If we select the slot arms with a quarter wavelength difference in length, i.e., $kL_{x'} - kL_{y'} = \pi/2$ ($kL_{x'} = \pi/2$ and $kL_{y'} = 0$), then the right circularly polarized component of the reflected wave is eliminated and the remaining left circularly polarized component becomes:

$$\vec{E}^{refl} = (\hat{u}_x - j\hat{u}_y)\, a e^{jkz} e^{2j\psi} e^{-j\omega t} \quad (8)$$

From Eqs. (1) and (8), we notify that the reflected waves have been delayed in phase by 2ψ due to element rotation by an angle ψ. In addition, the full period (360°) is satisfied when the angle of rotation is 180°.

3. ELEMENT ANALYSIS AND DESIGN

The CP reflectarray performance depends on the cell characteristics (phase and amplitude). As a result, the cells are optimized to satisfy circular polarization requirements (axial ratio, gain, etc.). The infinite array is illuminated by a normal incident Left-hand CP (LHCP) plane wave. The LHCP is considered as the co-polarized wave while the RHCP is cross-polarized. Investigation and verification are performed using full wave package [16]. The reflectarray element's size is a quarter wavelength size of $2.5 \times 2.5\,\text{mm}^2$ at 30 GHz. The substrate is FR4 with $\varepsilon_r = 4.5$, loss tangent 0.05 and thickness 0.8128 mm fully backed by conducting ground plane.

3.1. Polygonal Stubs Patch Reflectarray Cell

A new schematic is proposed by attaching a circular patch with four polygonal stubs having fixed phase distribution (0 90 0 90) degrees. That phase distribution can be obtained using four stubs differing in lengths by quarter wavelength, i.e., stubs 1 and 3 have the same length L_1 while stubs 2 and 4 have $L_1 + \lambda/4$. The cell schematic is shown in Fig. 2. The angular rotation technique will be used for obtaining the required reflected phase. The radius of the patch is 0.55 mm with stub widths of 0.2 mm. The stub lengths are 0.3 mm and 1.26 mm, respectively.

3.2. Butterfly Reflectarray Cell

The upper surface of the cell has a longitudinal bowtie printed strip with intermediating two arc strips. The inner and outer radii of the arc strips are 0.65 mm and 0.95 mm, respectively. The length of the bowtie strip is 1.8 mm with narrower and wider widths of 0.2 mm and 0.5 mm, respectively as shown in Fig. 3.

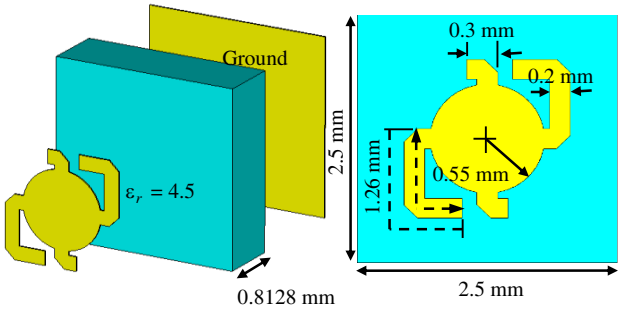

Figure 2. Polygonal stubs patch CP reflectarray cell.

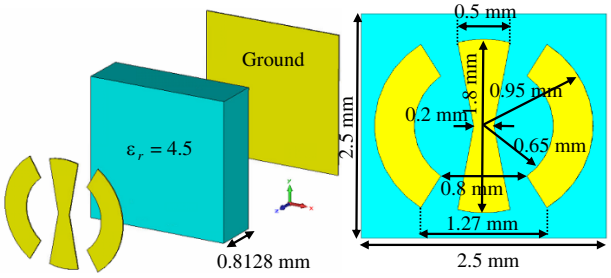

Figure 3. Butterfly CP reflectarray cell.

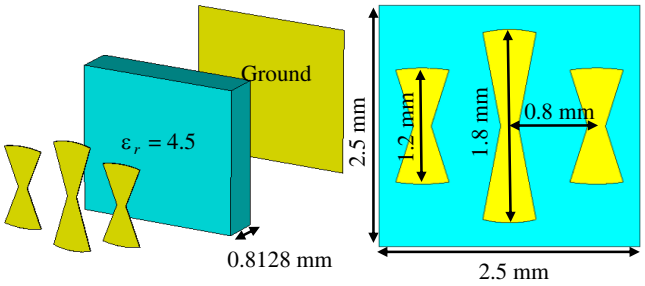

Figure 4. Triple bowtie CP reflectarray cell.

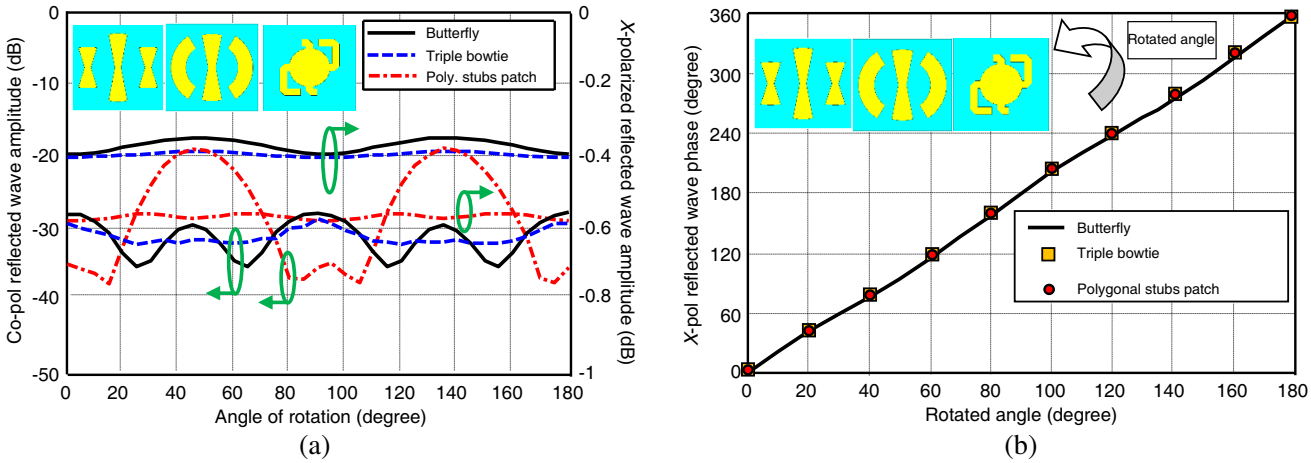

Figure 5. The co-polar and cross-polar reflected fields for the three different cell types at 30 GHz. (a) Magnitude. (b) Phase.

3.3. Triple Bowtie Reflectarray Cells

The upper conductor is modified by changing the two arc strips with two bowtie-dipoles of the same length.

The ratio of the small dipole to length of the centered one was optimized at 30 GHz to obtain acceptable cross- and co-polarized waves of unit cell. The cell schematic is shown in Fig. 4. The distance between the dipoles is 0.8 mm with the same outer and inner widths of 0.2 mm and 0.5 mm, respectively. The small dipole length is 1.2 mm while the centered one is 1.8 mm.

The dimensions of the butterfly-shaped, triple bowtie and polygonal stubs patch cells are optimized to satisfy minimal cross-polarized ratio (reflected LHCP to incident LHCP ratio) below -20 dB. In addition, co-polarized ratio (reflected RHCP to incident LHCP ratio) is better than -0.6 dB at 30 GHz. To assess the cell performance for the reflectarray within the desired band, the reflected co-polar and cross-polar are shown in Fig. 5 at 30 GHz where the magnitude is shown in Fig. 5(a) and the phase shown in Fig. 5(b) satisfying the 360° with linear variation.

3.4. Reflectarray Analysis and Design

A center-fed reflectarrays are designed at 30 GHz. The reflectarray is designed as a broadside radiator. Considering that the reflectarray in the x-y plane is illuminated by a feed with a phase center located at (x_f, y_f, z_f), the required phase compensation, $\Phi\ (x_i, y_i)$, at each element of the array to collimate a beam in the (θ_o, φ_o) direction is determined as:

$$\begin{aligned} \Phi(x_i, y_i) &= k_o\left(d_i - \sin\theta_o(x_i\cos\phi_o + y_i\sin\phi_o)\right) \\ d_i &= \sqrt{(x_i - x_f)^2 + (y_i - y_f)^2 + (z_f)^2} \end{aligned} \tag{9}$$

where k_o is the propagation constant in the free space, d_i the distance from the feed phase center location to the element i of the array, and (x_i, y_i) are the coordinates of the cell center. They are built based on the required phase compensation at each cell. The array is constructed of $25 \times 25(625)$ elements of physical area $62.5 \times 62.5\,\text{mm}^2$ $(6.25\lambda_o \times 6.25\lambda_o)$. The focal length is determined based on a $-10\,\text{dB}$ edge tapering at 30 GHz, which is found to be 40 mm.

3.5. Reflectarray Numerical Versus Measured Results

Practically, the reflectarray and horn are supported by aluminum bars fixed on a rotating tower of the anechoic chamber for far-field measurements. As a result, the simulated models include these supports and are illustrated in Fig. 6. The sketch of the three reflectarray models and their photos are shown in the same figure. The same feeder is used with all reflectarrays. A compact size dual-mode circularly polarized horn is optimized using the commercial software CST [16] and used as a feed for the reflectarray [17].

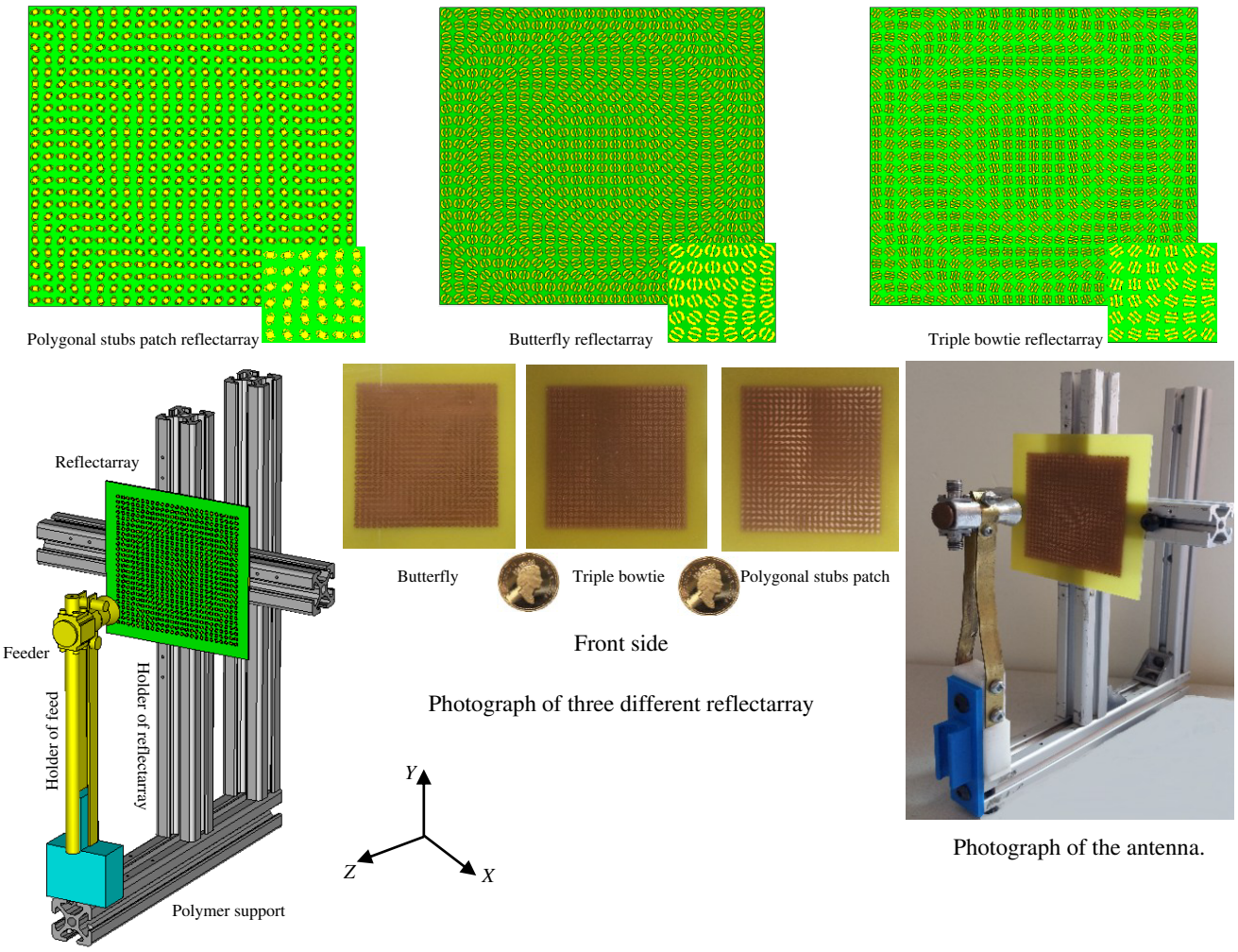

Figure 6. Sketch for the simulated reflectarray layouts with its support and feed and the photo of different reflect array and a photo of the actual antenna.

3.5.1. Reflectarray Feed Matching Results

The substrate frame facilitates fixing the reflectarray on the holding kit by 2 screws as illustrated in Fig. 6. The reflection coefficients of reflectarrays are shown in Figs. 7, 8 and 9 for polygonal stubs patch,

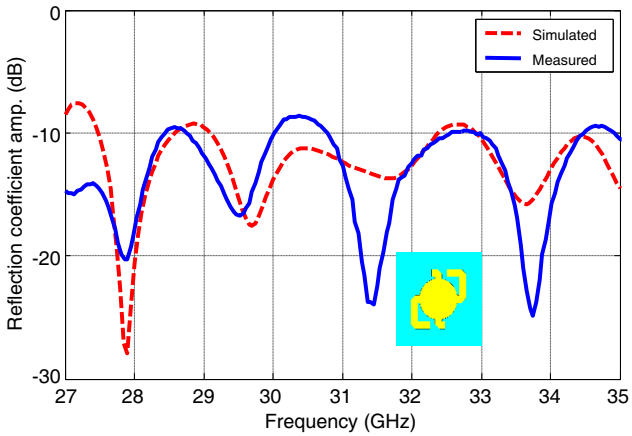

Figure 7. Polygonal stubs patch reflectarray reflection coefficient.

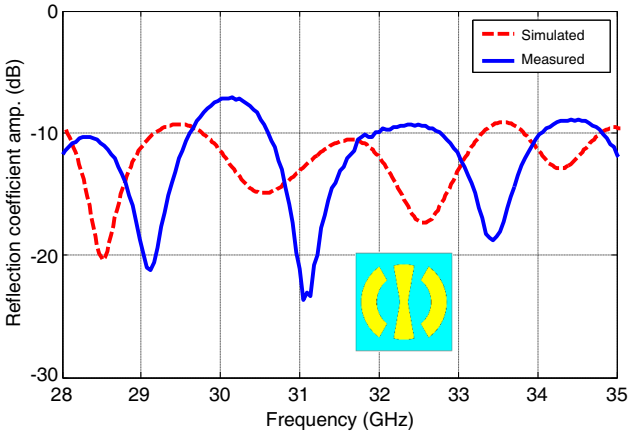

Figure 8. Butterfly reflectarray reflection coefficient.

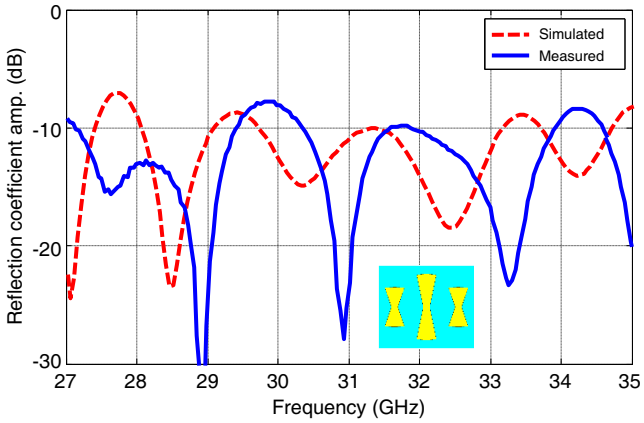

Figure 9. Triple bowtie reflectarray reflection coefficient.

butterfly and three dipoles of bowtie shape, respectively. In the center fed case, the feeder interaction with the reflectarray causes standing waves between the feeder and the reflectarray, which affect the feeder matching. The effect of each reflector is slightly different from each other.

3.5.2. Far-Field Pattern Results

The structure is fixed on a mechanical rotator by two screws, and the coaxial cable carrying the transmit signal is plugged in the feed connector as illustrated below. For accurate measurements, the structure is aligned carefully with the anechoic chamber receiving rectangular waveguide probe. Since the reflectarray is center fed by the horn with its connected coaxial cable supported by metallic strip holder, there is an extra blockage which degrades the side-lobes level in x-z plane. Furthermore, the effect of existing coaxial cable in the lower half parts of the array makes the y-z plane pattern asymmetric. The measured far-field patterns are in good agreement with simulated ones as shown in Figs. 10, 11 and 12, respectively, for each model.

3.5.3. Axial Ratio Results

The axial ratio of circularly polarized antenna is the ratio of right-hand circular polarization (RHCP) to left-hand circular polarization (LHCP) or vice versa. For considerable circularly polarized antennas, it defines the limitation of AR to be beyond 3 dB. The axial ratio of each reflectarray model is measured and compared with simulated one. There are some difference due to inaccurate fabricated dimensions

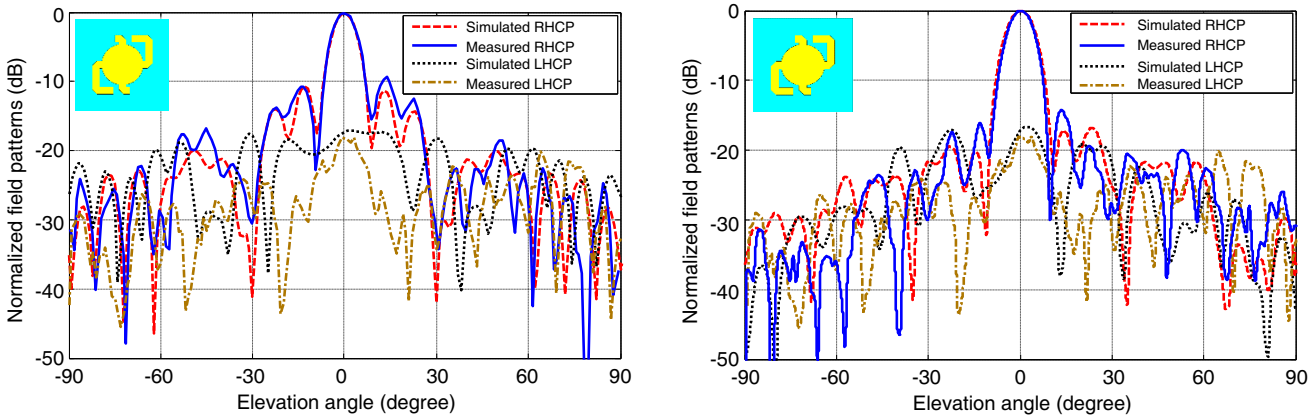

Figure 10. Measured and computed far field co-polar and cross-polar radiation patterns of the polygonal stubs patch reflectarray in x-z and y-z planes at 30 GHz. (a) x-z plane. (b) y-z plane.

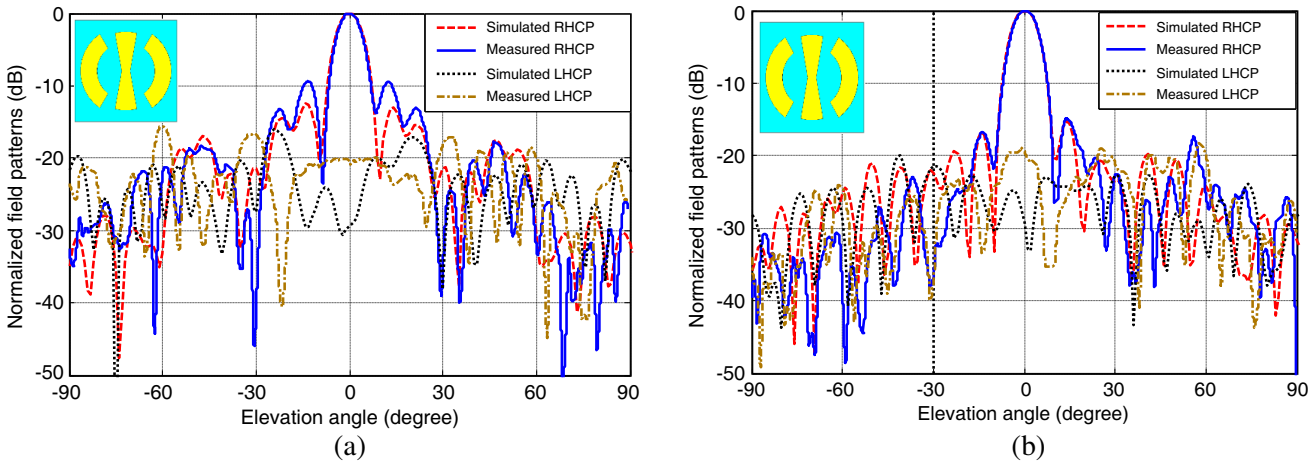

Figure 11. Measured and computed far field co-polar and cross-polar radiation patterns of the butterfly reflectarray in x-z and y-z planes at 30 GHz. (a) x-z plane. (b) y-z plane.

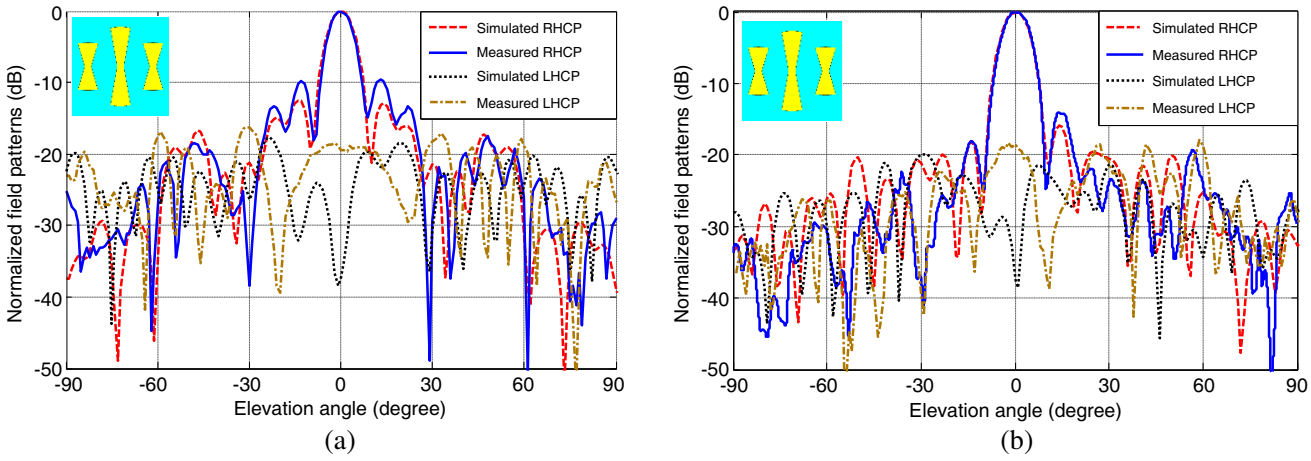

Figure 12. Measured and computed far field co-polar and cross-polar radiation patterns of the triple bowtie reflectarray in x-z and y-z planes at 30 GHz. (a) x-z plane. (b) y-z plane.

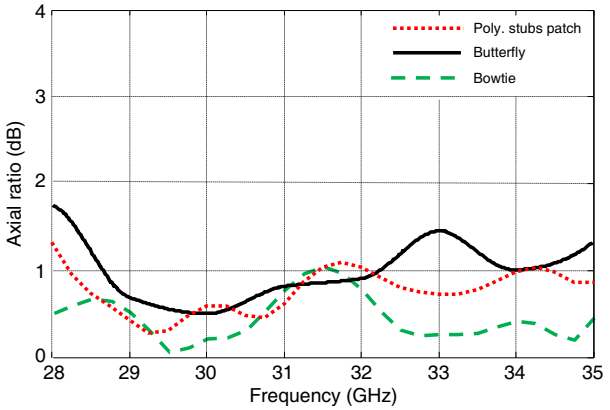

Figure 13. Simulated axial ratio versus frequency.

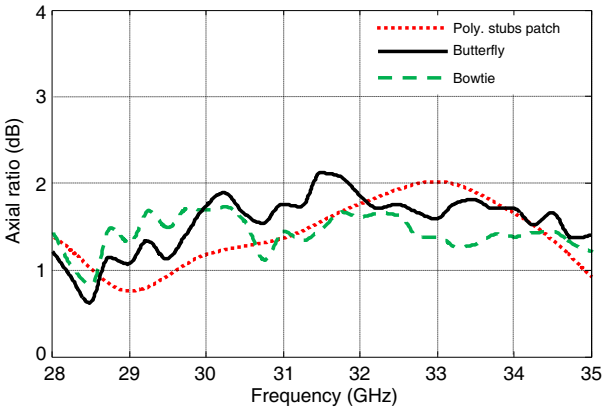

Figure 14. Measured axial ratio versus frequency.

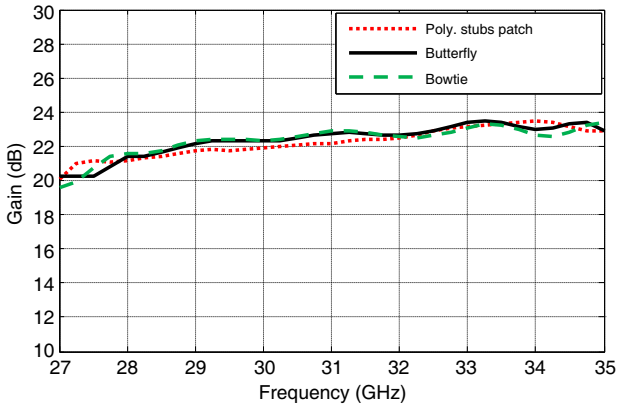

Figure 15. Gain versus frequency.

of the horn septum, septum misaligned vertically, i.e., the septum is tilted a bit from the y-axis. In addition, the position of the horn is not in the center of the reflectarray at measuring process. In addition, the tolerance of reflectarray fabrication process can also be included. Figs. 13 and 14 explore the simulated and measured axial ratios versus frequency, respectively. Both results are beyond 3 dB for all models, which make reflectarrays as considerable CP antennas. The gain plot is illustrated in Fig. 15. The gain level is varied from 20 dB at 27 GHz to 23.4 dB at 35 GHz. The 1.5 dB gain variation bandwidth is about 13.3%. The bowtie and butterfly reflectarray gain plots are almost the same since cell CP characteristics of both models are similar to that illustrated in Fig. 5. While the CP behavior of polygonal stubs patch cell is a bit worse than the two former models, its gain level is decreased by 0.5 dB compared with butterfly and bowtie reflectarrays' gains around 30 GHz.

4. CONCLUSIONS

Three low profile CP Reflectarray models are presented in this paper and designed using the angular rotation technique. The performances of the fabricated models are compared with full wave analysis at 30 GHz. A conical horn with septum, converting the linearly polarization wave to circular polarization in the operating band, is used to illuminate the RA elements. The quadruple wavelength elements have been used in the RA designs, for avoiding grating lobes. By comparative analysis on the measured performance of the proposed antennas, it is observed that the reflectarrays provide wide axial ratio bandwidth, with level less than 2 dB in the operating band. The measured antennas' performance shows good agreement with simulation.

ACKNOWLEDGMENT

This work is performed at Concordia University.

REFERENCES

1. Elbert, B., *Introduction to Satellite Communication*, Artech House, 2008.
2. Chaharmir, M. R., J. Shaker, M. Cuhaci, and A. Sebak, "Circularly polarised reflectarray with cross-slot of varying arms on ground plane," *Electronics Letters*, Vol. 38, No. 24, 2002.
3. Guo, L., P. Tan, and T. Chio, "A simple approach to achieve polarization diversity in broadband reflectarrays using single-layered rectangular patch elements," *Microwave and Optical Technology Letters*, Vol. 47, No. 2, 305–310, Feb. 2015.
4. Zhao, G., Y. C. Jiao, F. Zhang, and F. S. Zhang, "A subwavelength element for broadband circularly polarized reflectarrays," *IEEE Antennas and Wireless Propag. Lett.*, Vol. 9, 2010.
5. Albooyeh, M., N. Komjani, and M. S. Mahani, "Circularly polarized element for reflectarray antennas," *IEEE Antennas and Wireless Propag. Lett.*, Vol. 8, 319–322, 2009.
6. Abd-Elhady, A. M., S. H. Zainud-Deen, A. A. Mitkees, and A. A. Kishk, "Linearly polarized fed circularly polarized DRA reflectarray," *International Journal of Electromagnetics and Applications*, Vol. 2, No. 2, 11–15, 2012.
7. Ren, L., Y.-C. Jiao, F. Li, J.-J. Zhao, and G. Zhao, "A dual-layer T-shaped element for broadband circularly polarized reflectarray with linearly polarized feed," *IEEE Antennas and Wireless Propag. Lett.*, Vol. 10, 407–410, 2011.
8. Zainud-Deen, S. H., A. M. Abd-Elhady, A. A. Mitkees, and A. A. Kishk, "Design of dielectric resonator reflectarray using full-wave analysis," *26th National Radio Science Conference (NRSC 2009)*, 1–9, Faculty of Engineering, Future Univ., Egypt, Mar. 2009.
9. Huang, J. and R. J. Pogorzelski, "A Ka-band microstrip reflectarray with variable rotation angles," *IEEE Trans. Antennas Propag.*, Vol. 46, No. 5, 650–656, May 1998.
10. Han, C., J. Huang, and K. Chang, "A high efficiency offset-fed X/Ka dual band reflectarray using thin membranes," *IEEE Trans. Antennas Propag.*, Vol. 53, No. 9, 2792–2797, Sep. 2005.
11. Strassner, B., C. Han, and K. Chang, "Circularly polarized reflectarray with microstrip ring elements having variable rotation angles," *IEEE Trans. Antennas Propag.*, Vol. 52, No. 4, 1122–1125, 2004.
12. Srinivasan, V. and V. F. Fusco, "Circularly polarized mechanically steerable reflectarray," *Inst. Elect. Eng. Proc. Microw. Antennas Propag.*, Vol. 152, No. 6, 511–514, Dec. 2005.
13. Yu, A., F. Yang, A. Z. Elsherbeni, J. Huang, and Y. Kim, "An offset-fed X-band reflectarray antenna using a modified element rotation technique," *IEEE Trans. Antennas Propag.*, Vol. 60, No. 3, 1619–1624, Mar. 2012.
14. Zhao, M.-Y., G.-Q. Zhang, X. Li, J.-M. Wu, and J.-Y. Shang, "Design of new single-layer multiple-resonance broadband circularly polarized reflectarrays," *IEEE Antennas and Wireless Propag. Lett.*, Vol. 12, 356–359, 2013.
15. Mohamoud, A. and A. Kishk, "Ka-band dual mode circularly polarized reflectarray," *IEEE Conference ANTEM 2014*, Victoria, Canada, 2014.
16. CST microwave studio, www.cst.com, 2015.
17. http://www.ok1dfc.com/eme/technic/septum/ra3aq.pdf.